CLEO CONF 02-08
ICHEP02 ABS933

Preliminary Results on $|V_{ub}|$ from Inclusive Semileptonic B Decays with Neutrino Reconstruction*

A. Bornheim,[1] E. Lipeles,[1] S. P. Pappas,[1] A. Shapiro,[1] W. M. Sun,[1] A. J. Weinstein,[1] R. Mahapatra,[2] R. A. Briere,[3] G. P. Chen,[3] T. Ferguson,[3] G. Tatishvili,[3] H. Vogel,[3] N. E. Adam,[4] J. P. Alexander,[4] K. Berkelman,[4] V. Boisvert,[4] D. G. Cassel,[4] P. S. Drell,[4] J. E. Duboscq,[4] K. M. Ecklund,[4] R. Ehrlich,[4] L. Gibbons,[4] B. Gittelman,[4] S. W. Gray,[4] D. L. Hartill,[4] B. K. Heltsley,[4] L. Hsu,[4] C. D. Jones,[4] J. Kandaswamy,[4] D. L. Kreinick,[4] A. Magerkurth,[4] H. Mahlke-Krüger,[4] T. O. Meyer,[4] N. B. Mistry,[4] E. Nordberg,[4] J. R. Patterson,[4] D. Peterson,[4] J. Pivarski,[4] D. Riley,[4] A. J. Sadoff,[4] H. Schwarthoff,[4] M. R. Shepherd,[4] J. G. Thayer,[4] D. Urner,[4] G. Viehhauser,[4] A. Warburton,[4] M. Weinberger,[4] S. B. Athar,[5] P. Avery,[5] L. Breva-Newell,[5] V. Potlia,[5] H. Stoeck,[5] J. Yelton,[5] G. Brandenburg,[6] D. Y.-J. Kim,[6] R. Wilson,[6] K. Benslama,[7] B. I. Eisenstein,[7] J. Ernst,[7] G. D. Gollin,[7] R. M. Hans,[7] I. Karliner,[7] N. Lowrey,[7] C. Plager,[7] C. Sedlack,[7] M. Selen,[7] J. J. Thaler,[7] J. Williams,[7] K. W. Edwards,[8] R. Ammar,[9] D. Besson,[9] X. Zhao,[9] S. Anderson,[10] V. V. Frolov,[10] Y. Kubota,[10] S. J. Lee,[10] S. Z. Li,[10] R. Poling,[10] A. Smith,[10] C. J. Stepaniak,[10] J. Urheim,[10] Z. Metreveli,[11] K.K. Seth,[11] A. Tomaradze,[11] P. Zweber,[11] S. Ahmed,[12] M. S. Alam,[12] L. Jian,[12] M. Saleem,[12] F. Wappler,[12] E. Eckhart,[13] K. K. Gan,[13] C. Gwon,[13] T. Hart,[13] K. Honscheid,[13] D. Hufnagel,[13] H. Kagan,[13] R. Kass,[13] T. K. Pedlar,[13] J. B. Thayer,[13] E. von Toerne,[13] T. Wilksen,[13] M. M. Zoeller,[13] H. Muramatsu,[14] S. J. Richichi,[14] H. Severini,[14] P. Skubic,[14] S.A. Dytman,[15] J.A. Mueller,[15] S. Nam,[15] V. Savinov,[15] S. Chen,[16] J. W. Hinson,[16] J. Lee,[16] D. H. Miller,[16] V. Pavlunin,[16] E. I. Shibata,[16] I. P. J. Shipsey,[16] D. Cronin-Hennessy,[17] A.L. Lyon,[17] C. S. Park,[17] W. Park,[17] E. H. Thorndike,[17] T. E. Coan,[18] Y. S. Gao,[18] F. Liu,[18] Y. Maravin,[18] R. Stroynowski,[18] M. Artuso,[19] C. Boulahouache,[19] K. Bukin,[19] E. Dambasuren,[19] K. Khroustalev,[19] R. Mountain,[19] R. Nandakumar,[19] T. Skwarnicki,[19] S. Stone,[19] J.C. Wang,[19] A. H. Mahmood,[20] S. E. Csorna,[21] I. Danko,[21] G. Bonvicini,[22] D. Cinabro,[22] M. Dubrovin,[22] and S. McGee[22]

(CLEO Collaboration)

[1]*California Institute of Technology, Pasadena, California 91125*
[2]*University of California, Santa Barbara, California 93106*
[3]*Carnegie Mellon University, Pittsburgh, Pennsylvania 15213*
[4]*Cornell University, Ithaca, New York 14853*
[5]*University of Florida, Gainesville, Florida 32611*
[6]*Harvard University, Cambridge, Massachusetts 02138*
[7]*University of Illinois, Urbana-Champaign, Illinois 61801*
[8]*Carleton University, Ottawa, Ontario, Canada K1S 5B6*
and the Institute of Particle Physics, Canada M5S 1A7
[9]*University of Kansas, Lawrence, Kansas 66045*
[10]*University of Minnesota, Minneapolis, Minnesota 55455*
[11]*Northwestern University, Evanston, Illinois 60208*
[12]*State University of New York at Albany, Albany, New York 12222*
[13]*Ohio State University, Columbus, Ohio 43210*
[14]*University of Oklahoma, Norman, Oklahoma 73019*

[15] *University of Pittsburgh, Pittsburgh, Pennsylvania 15260*
[16] *Purdue University, West Lafayette, Indiana 47907*
[17] *University of Rochester, Rochester, New York 14627*
[18] *Southern Methodist University, Dallas, Texas 75275*
[19] *Syracuse University, Syracuse, New York 13244*
[20] *University of Texas - Pan American, Edinburg, Texas 78539*
[21] *Vanderbilt University, Nashville, Tennessee 37235*
[22] *Wayne State University, Detroit, Michigan 48202*
(Dated: July 23, 2002)

Abstract

We present an analysis of the composition of inclusive semileptonic B meson decays using 9.4 fb^{-1} of e^+e^- data taken with the CLEO detector at the $\Upsilon(4S)$ resonance. In addition to measuring the charged lepton kinematics, the neutrino 4-vector is inferred using the hermeticity of the detector. We perform a maximum likelihood fit over the full three-dimensional differential decay distribution for the fractional contributions from the $B \to X_c l\nu$ processes with $X_c = D$, D^*, D^{**}, and non-resonant X_c, and the process $B \to X_u l\nu$. From the fit results we extract $|V_{ub}| = (4.05 \pm 0.18 \pm 0.58 \pm 0.25 \pm 0.21 \pm 0.56) \times 10^{-3}$ where the errors are statistical, detector systematics , $B \to X_c l\nu$ model dependence, $B \to X_u l\nu$ model dependence, and theoretical uncertainty respectively.

*Submitted to the 31st International Conference on High Energy Physics, July 2002, Amsterdam

I. INTRODUCTION

The CKM matrix element $|V_{ub}|$ is the coupling between the bottom and up quarks, and is therefore a fundamental parameter in the Standard Model. Its value is relevant to studies of flavor-changing currents, including the rates of B and B_s mixing and CP violation in the mixing and decays of B hadrons.

Recent theoretical progress in charmless semileptonic B decays using Heavy Quark Effective Theory (HQET) and the Operator Product Expansion (OPE) [1–4] has made possible new levels of precision in the measurement of $|V_{ub}|$[5]. The calculations relate $|V_{ub}|$ to the partial branching fraction of $B \to X_u l\nu$ in a restricted region of phase space in which $B \to X_c l\nu$ does not contribute. The region of phase space most accessible to experiment is the lepton energy endpoint, $E_\ell > (m_B^2 - m_D^2)/2m_B$. This region was used in the first measurement of $B \to X_u l\nu$ establishing a non-zero value of $|V_{ub}|$[6]. Unfortunately the OPE calculation is not valid in the very restricted region of phase space delineated by this lepton energy cut. A recent CLEO measurement has used a spectral function measured in $B \to X_s\gamma$ to obtain the normalization factor which relates the measured partial branching fraction in the lepton endpoint region to $|V_{ub}|$[5]. Another method is to replace the lepton energy cut with a cut on the invariant mass of the lepton pair[2, 3], q^2, or on the mass of the recoiling hadronic system, M_X, to exclude $B \to X_c l\nu$ events. Recent theoretical work suggests that a combination of cuts on both q^2 and M_X yields the smallest uncertainty[4].

In this paper we report an analysis of $B \to Xl\nu$ decays in which both the charged lepton and the neutrino are reconstructed. The neutrino is reconstructed using the approximate hermeticity of the CLEO II and CLEO II.V detectors and the well known initial state of the e^+e^- system produced by the Cornell Electron Storage Ring (CESR). The q^2 kinematic variable is then calculated directly, and the M_X kinematic variable can be calculated if the B momentum, $\vec{p}_B$, is known,

$$M_X^2 \;=\; M_B^2 + q^2 - 2E_{beam}(E_\ell + E_\nu) + 2|\vec{p}_B||\vec{p}_{\ell\nu}|\cos\theta_{B\cdot\ell\nu},$$

where $\vec{p}_{\ell\nu}$ is the sum of the charged lepton and neutrino momenta and $\theta_{B\cdot\ell\nu}$ is the angle between $\vec{p}_{\ell\nu}$ and the B momentum direction. Since the B mesons are the daughters of an $\Upsilon(4S)$ produced at rest, the magnitude of the B momentum is known and small, however its direction is unmeasured. The last term in the M_X^2 equation depends on the B momentum direction, and is small, unmeasured, and neglected in this analysis. From the lepton pair sample, the differential decay rate is measured as a function of the reconstructed quantities q^2, M_X, and E_ℓ. The experimental resolution on the neutrino four-momentum is poor, with a narrow core of approximately 120 MeV and broad tail of over-estimation of the neutrino energy which extends up to 1.5 GeV. The resulting resolution on q^2 and M_X is also poor, so it is not possible to cleanly isolate $B \to X_u l\nu$ events with cuts on these variables. Instead, we fit this observed distribution to a sum of models for the different hadronic final states: D, D^*, D^{**}, X_c non-resonant, and X_u. From the fit results we infer the partial branching fraction over a region of phase space with high q^2 and low M_X. These partial branching fractions are related to $|V_{ub}|$ by theoretical calculations whose uncertainty has been estimated [4].

The data were accumulated with two configurations of the CLEO detector [7], CLEO II and CLEO II.V, with an integrated luminosity of 9.4 fb^{-1} taken on the $\Upsilon(4S)$ resonance and an additional 4.5 fb^{-1} taken off resonance, just below the $B\overline{B}$ production threshold. Both configurations cover 95% of the 4π solid angle with drift chambers and a cesium iodide calorimeter. In addition there are muon chambers with measurements made at 3, 5, and 7 hadronic interaction lengths of iron and a time of flight system which augments the particle ID information from specific ionization (dE/dx). In the the CLEO II configuration, there were three concentric drift chambers filled with a mixture of argon and ethane. In the CLEO II.V detector, the innermost tracking chamber was replaced with a three layer silicon detector and the drift chamber gas was changed to a mixture of helium and propane.

II. NEUTRINO RECONSTRUCTION AND EVENT SELECTION

Events are selected to have an electron or muon with momentum greater than 1 GeV/c and a well reconstructed neutrino. Additional cuts are used to suppress background events from the $e^+e^- \to q\overline{q}$ continuum.

The leptons are selected to fall within the barrel region of the detector ($|\cos\theta| < .71$, where θ is the angle between the lepton momentum and the beam axis). Electrons are selected based on E/p, dE/dx, and time of flight information combined using a likelihood technique. Muons are identified by requiring a penetration of 3 interaction lengths of iron for muons less than 1.5 GeV/c and 5 interaction lengths for muons greater than 1.5 GeV/c. The absolute lepton identification efficiencies are calculated by embedding leptons from radiative QED events into hadronic events. The rate at which pions and kaons fake leptons is measured by reconstructing $K_S^0 \to \pi^+\pi^-$, $D^0 \to K^-\pi^+$, and $\bar{D^0} \to K^+\pi^-$ without using particle identification and then checking daughter particle lepton identification signatures.

Neutrinos are reconstructed by subtracting all observed track and neutral shower four-momenta from the four-momentum of the e^+e^- initial state which is at rest in the laboratory,

$$p_\nu^\mu = p_{e^+e^-}^\mu - p_{visible}^\mu.$$

The errors made in this assumption are due to particles lost through inefficiency or acceptance, fake tracks and showers, and other undetected particles such as second neutrinos, K_L^0's, or neutrons. Several cuts are made to select events in which these effects are reduced and the neutrino four-momentum resolution is correspondingly enhanced. Since extra neutrinos are correlated with extra leptons, events with a lepton beyond the signal lepton in the event are rejected.

The primary source of fake tracks is from charged particles which do not have sufficient transverse momentum, p_t, to reach the calorimeter and therefore curl multiple times in the tracking chambers. The portions of the track after the initial outbound section may accidentally be called a second track. Criteria have been developed to identify such errors and make a best estimate of the actual charged particles in the event. Events for which the total charge of the tracks is not zero are removed, reducing the effect of lost or fake tracks. Showers in the calorimeter associated with tracks in the drift chamber are removed, so as not to double count their energy. The association between tracks and showers has been refined to take into account secondary hadronic showers which can appear to be showers isolated from tracks. Finally a requirement is made that the ratio of the reconstructed neutrino four-momentum divided by twice the reconstructed neutrino energy be less than 0.35 GeV, $\frac{M_{missing}^2}{2E_\nu} < .35$ GeV. This quantity is constructed to be proportional to the energy of a lost or fake particle. The reconstructed neutrino's energy is assigned to be the magnitude of the momentum, because the momentum is not dependent on the particle identification of the tracks and so has a better resolution than the direct energy measurement.

Continuum events are suppressed by a combination of event shape and orientation variables which exploit the fact that continuum events tend to be jet-like and aligned with the beam axis, whereas $B\overline{B}$ events are more spherical and their orientation is uniformly distributed in the detector. The second Fox-Wolfram moment [8], R2, of the energy flow in the event is required to be less than 0.4. In addition a neural network is used to combine R2, the angle between the lepton and the thrust axis, the angle between the lepton and the beam axis, and the fraction of the energy lying in 9 separate cones around the lepton direction, which cover the full the 4π solid angle. The R2 cut is more than 99% and 95% efficient for $B \to X_c l\nu$ and $B \to X_u l\nu$ respectively, while removing 60% of the continuum events. The neural net cut removes an additional 73% of the continuum background while keeping 92% and 94% of the $B \to X_c l\nu$ and $B \to X_u l\nu$ respectively.

After all cuts we observe 42333 events from CLEO II and 81368 events from CLEO II.V. The overall efficiency varies from 1.5% for $B \to X_c l\nu$ non-resonant to 4.2% for $B \to X_u l\nu$.

III. FITTING FOR COMPOSITION

The full three dimensional differential decay rate distribution as a function of the reconstructed quantities q^2, M_X, and E_ℓ is fit for the contributions of the signals and backgrounds. The signals are $B \to Dl\nu$, $B \to D^*l\nu$, $B \to D^{**}l\nu$, $B \to X_c l\nu$ non-resonant, and $B \to X_u l\nu$. The backgrounds are events where the B decay candidate is faked by a lepton from the process $b \to c \to X\ell\nu$, a lepton from the $e^+e^- \to q\overline{q}$ continuum, or a fake lepton. We have the freedom to choose the kinematic variables used in the fit. We use $q^2/(E_\ell + E_\nu)^2$, M_X, and $\cos\theta_{W\ell}$. The helicity angle of the virtual W, $\cos\theta_{W\ell}$, is defined to be the angle between the lepton momentum in the W frame and the W in the lab frame. The fit variables have been chosen to minimize complexity of the phase space boundaries and cover the same kinematic space as q^2, E_ℓ, and E_ν.

We perform a binned maximum-likelihood fit where the probability distribution functions (PDFs) are constructed from weighted Monte Carlo or data events. The fit uses electrons and muons simultaneously, with a separate set of PDFs for the electrons and muons. The likelihood is implemented to take into account the PDF statistics using the method described in reference [9]. The projections of the reconstructed quantities q^2, M_X, and $\cos\theta_{W\ell}$ of the various $B \to Xl\nu$ modes are shown in Figure 1. Projections of the fit result are shown in Figure 2. Projections restricted to the region of enhanced $B \to X_u l\nu$ sensitivity are shown in Figure 3. It should be noted that the correlations between the the three variables shown in the projections are fully included in the fit, and provide considerable power in distinguishing the contributions of the various components.

The $B \to Xl\nu$ modes, secondary leptons and real leptons from continuum are simulated with CLEO's GEANT based Monte Carlo. The $B \to Dl\nu$ and $B \to D^{**}l\nu$ modes are modeled with ISGW2 [10]. The $B \to D^*l\nu$ mode is modeled with HQET using CLEO's previous measurement of the form factors [11]. The X_c non-resonant modes are modeled with a combination of the Goity and Roberts model[12] and a crude model of $B \to \Lambda_c X l\nu$. For an assessment of the $B \to X_c l\nu$ model dependence, the $B \to Dl\nu$ and $B \to D^*l\nu$ form factors are varied within their experimentally allowed ranges, and the $B \to D^{**}l\nu$ masses are varied in an ad-hoc manner. Because very little is known about the X_c non-resonant mass spectrum, it is reweighted drastically in the study of the $B \to X_c l\nu$ model dependence. In a further study, each X_c final state is constrained to a value away from the nominal fit result. The results of the variations are summed in quadrature. The modeling of the $B \to X_u l\nu$

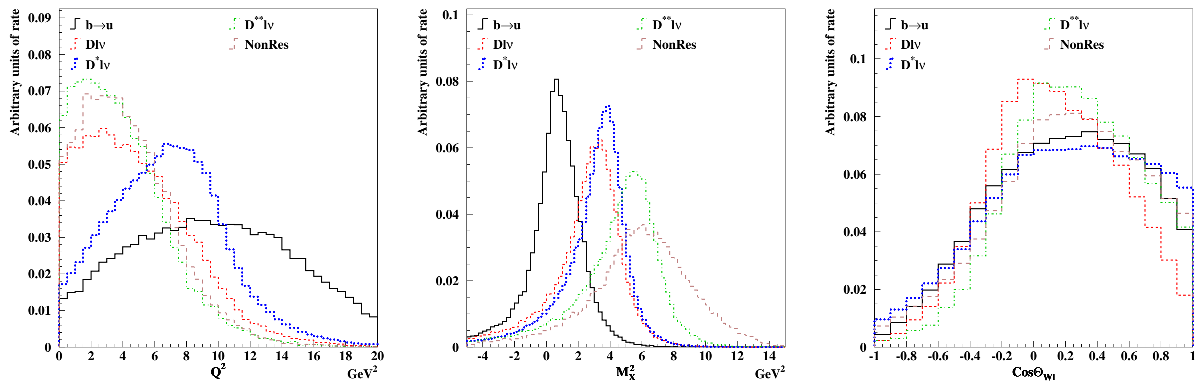

FIG. 1: Distributions of the various $B \to Xl\nu$ modes as functions of the reconstructed quantities (left to right) q^2, M_X^2, and $\cos\theta_{W\ell}$. The modes are $B \to X_u l\nu$ (solid), $B \to Dl\nu$ (short dash), $B \to D^* l\nu$ (dots), $B \to D^{**} l\nu$ (dot-dash), and $B \to X_c l\nu$ non-resonant (long dash).

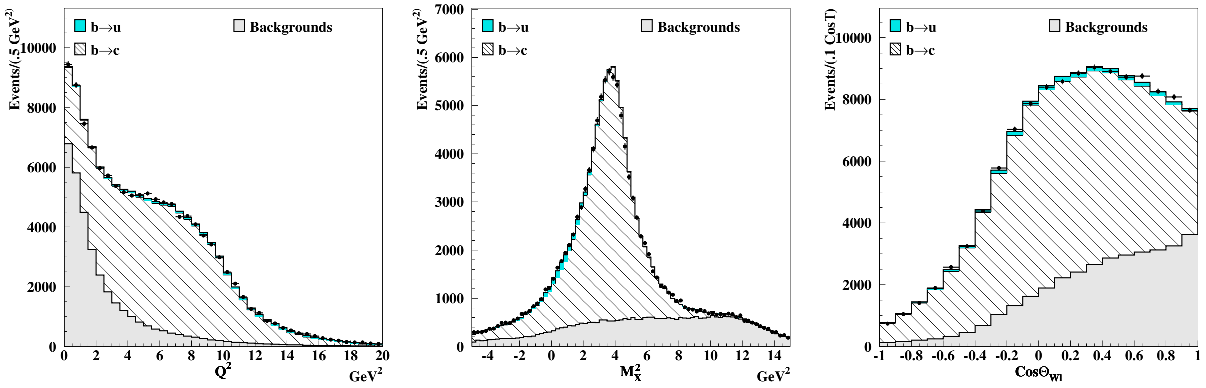

FIG. 2: Projections of the fit results in in the reconstructed quantities (left to right) q^2, M_X^2, and $\cos\theta_{W\ell}$. The solid histogram on the bottom is the sum of the backgrounds: continuum, secondary leptons, fake leptons. The hatched histogram is the sum of the $B \to X_c l\nu$ modes: $B \to Dl\nu$, $B \to D^* l\nu$, $B \to D^{**} l\nu$, and $B \to X_c l\nu$ non-resonant. The top histogram, barely visible, is the $B \to X_u l\nu$ component.

mode and the resulting model dependence is discussed in a later section.

The fake leptons are modeled by taking a sample of tracks from data that are classified as π, K, or μ (electrons and protons are not a significant source of fake leptons) and unfolding their spectra to get the true spectra of π, K and μ, which are then multiplied by the measured fake rates. This models fake leptons from both $B\overline{B}$ and $e^+e^- \to q\overline{q}$ continuum. The real leptons from continuum are modeled with continuum Monte Carlo which has been tuned to replicate the appropriate charm spectra. Charm is the source of most leptons from continuum. The models of both continuum and fakes have been validated and constrained by a comparison with the 4.5 fb^{-1} of off-resonance data. The secondary leptons are modeled with a convolution of CLEO's measured charm spectra from $B\overline{B}$ events and DELCO results on the inclusive semileptonic decays of charm[13].

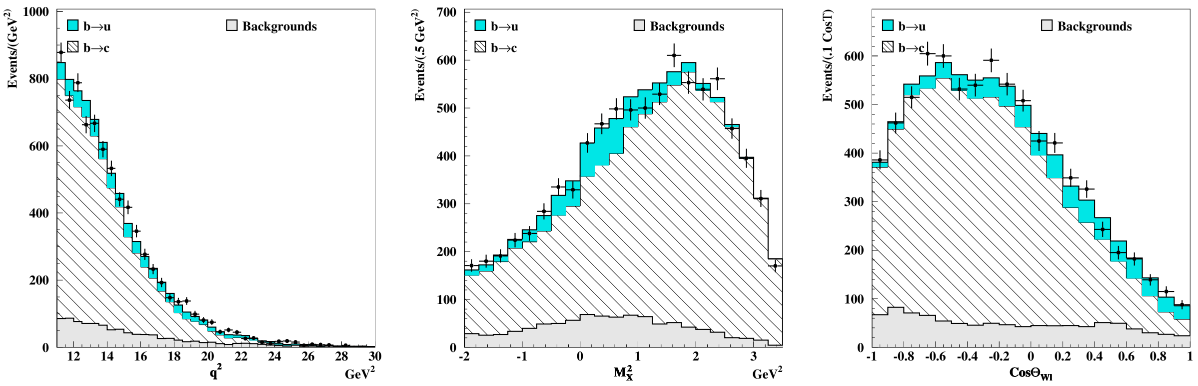

FIG. 3: Projections of the fit results in reconstructed quantities q^2, M_X^2, and $\cos\theta_{W\ell}$ with cuts of $q^2 > 11.0$ GeV$^2/c^4$ for the M_X^2 projection and $M_X^2 < 2.25$ GeV$^2/c^4$ for the q^2 . projection. The solid histogram on the bottom is the sum of the backgrounds: continuum, secondary leptons, fake leptons. The hatched histogram is the sum of the $B \to X_c l\nu$ modes: $B \to Dl\nu$, $B \to D^* l\nu$, $B \to D^{**} l\nu$, and $B \to X_c l\nu$ non-resonant. The top histogram, now clearly visible, is the $B \to X_u l\nu$ component.

The method of neutrino reconstruction adds a large amount of kinematic information to each event, however it also adds significant potential for systematic errors. The resolution on the neutrino kinematics is affected by the models of both the signal, the other B in the event, and the detector response. The GEANT Monte Carlo does not perfectly simulate the track and shower efficiencies and fake rates, nor are B decays well enough understood that the inclusive particle distributions are well known. For this analysis we employ a method of reweighting in order to quantify the effects of these uncertainties on our results. For example to study effect of the tracking efficiency uncertainty on result, the Monte Carlo events in which tracks are lost are given a higher or lower weight in constructing the PDFs and the fit is repeated. The scale of the variation made can in general be constrained by direct measurements of the quantity being varied. One important example is that having a K_L^0 in the event adds a tail to the neutrino resolution. The inclusive K_S^0 spectrum in $B\overline{B}$ events has been measured and can be used to constrain the K_L^0 spectrum.

IV. $B \to X_u l\nu$ MODEL DEPENDENCE

We use calculations based on HQET and the OPE to extract $|V_{ub}|$ from the $B \to X_u l\nu$ rate in restricted regions of phase space. This is a well controlled expansion and the theoretical uncertainties have been assessed by several authors [2–4]. However, the fit's region of sensitivity does not coincide with these regions, and, as previously mentioned, it is not possible to make cuts to isolate these regions, because of the poor resolution on the neutrino four-vector and hence q^2 and M_X^2. In order to calculate $|V_{ub}|$, we first make a model dependent inference of the partial branching fraction in a region, and then apply the HQET and OPE calculations. This prescription is designed to minimize the reliance on models and instead rely on the controlled expansion in HQET and OPE calculations.

$B \to X_u l\nu$ models are used for two purposes in this analysis. The first is in the simulation of the efficiency and resolution of the detector. This cannot be done with the HQET and OPE calculations, because they do not predict specific hadronic final states. The second use of models is to extrapolate and interpolate between the regions of high sensitivity to $B \to X_u l\nu$ and regions of interest for extracting $|V_{ub}|$. The fit is primarily sensitive to low M_X^2 and high q^2, but within this region the sensitivity is strongly biased toward the lepton energy end-point, hence the models are relied on to extrapolate to the full range of lepton energies.

The result of the fit is the fraction of $B \to X_u l\nu$ events in the sample. This is converted into a branching fraction using the efficiency determined by Monte Carlo simulation and number of $B\overline{B}$s in the sample. The $B \to X_u l\nu$ portion of the fit is driven by the region of phase space where the $B \to X_c l\nu$ contribution is not overwhelming, however the fit extrapolates from this region to the full space using the models. This results in a very large model dependence for the total rate. The effect can be reduced by calculating for each model a fraction, $f_{\rm region}^{\rm model}$, of events in a region of enhanced $B \to X_u l\nu$ sensitivity. The fractions, $f_{\rm region}^{\rm model}$, are calculated from the model using the true q^2 and M_X^2, not the reconstructed q^2 and M_X^2. The product of the branching fraction from the fit result for a model and $f_{\rm region}^{\rm model}$ is the inferred partial branching fraction of $B \to X_u l\nu$ for the model in region selected,

$$\Delta\mathcal{B}_{\rm region}^{\rm model} = \mathcal{B}(B \to X_u l\nu)^{\rm model} \times f_{\rm region}^{\rm model}.$$

$\Delta\mathcal{B}_{\rm region}^{\rm model}$ has significantly less dependence on the model than the inferred full branching fraction, $\mathcal{B}(B \to X_u l\nu)^{\rm model}$, however it still involves a model dependent combination of interpolation and extrapolation from the actual region of measurement.

The models used range across extremes from the ISGW2 model to a model with only non-resonant modes. The ISGW2 model contains only low mass hadronic resonances and no non-resonant or high mass hadronic systems. The purely non-resonant model implements the HQET and OPE prediction for the hadronic mass spectrum based on the $B \to X_s\gamma$ spectral function, where the hadronic system is decayed via JETSET. The true spectrum is likely somewhere between the extremes of all high mass non-resonant and all low mass resonances. Two permutations of the all non-resonant model correspond to changing the spectral function parameters, $\overline{\Lambda}$ and λ_1 within the bounds of the CLEO measurement [5]. Another model combines ISGW2 and some non-resonant events. In addition, the ISGW2 model is reweighted to have a higher or lower $\cos\theta_{W\ell}$, corresponding to more or less rate in the lepton end-point, or reweighted to have a harder or softer q^2 spectrum. Table I shows the results for the total rate and the inferred partial branching fractions for five different regions. The central value of $\Delta\mathcal{B}_{\rm region}$, reported in the first column of Table II, is the center of the range of models, and the model dependence uncertainty is assigned to cover the full range. The fit results for the branching fractions of the final states containing charm agree with previous CLEO measurements and will be reported in a subsequent paper.

In the context of HQET and the OPE another fraction, $f_{\rm region}^{\rm HQET}$, relates the partial branching fraction to $|V_{ub}|$[14],

$$|V_{ub}| = \left[3.07 \pm 0.12 \times 10^{-3}\right] \left[\frac{\Delta\mathcal{B}_{\rm region}}{.001 \times f_{\rm region}^{\rm HQET}} \frac{1.6{\rm ps}}{\tau_B}\right]^{1/2}.$$

The fractions, $f_{\rm region}^{\rm HQET}$, for the five regions used have been calculated with an evaluation of the theoretical uncertainty by Bauer *et al.* in reference [4]. Some of the regions have also been evaluated in reference[3]. The $|V_{ub}|$ results that correspond to the five inferred partial branching fractions with their respective model dependences are shown in Table II. We choose the $q^2 > 11$ GeV$^2/c^4$, $M_X < 1.5$ GeV$/c^2$ results as a central value because it has the least model dependence.

TABLE I: Dependence on the $B \to X_u l\nu$ model of the inferred total branching fraction, $\mathcal{B}(B \to X_u l\nu)$, and the inferred partial branching fractions, $\Delta\mathcal{B}^{\rm model}_{\rm region}$, for five regions. Entries are in units of 10^{-3}.

	ISGW2	ISGW2 & Non-Res	All Non-Resonant Nominal	Low $\overline{\Lambda}$,λ_1	High $\overline{\Lambda}$,λ_1	Harder q^2	Softer q^2	Higher $\cos\theta_{W\ell}$	Lower $\cos\theta_{W\ell}$
Total $\mathcal{B}(B \to X_u l\nu)$	0.996	1.211	1.808	2.289	1.620	0.803	1.159	0.956	1.039
$q^2 > 6$ GeV^2, $M_X < M_D$	0.629	0.686	0.835	0.859	0.811	0.582	0.655	0.606	0.653
$q^2 > 8$ GeV^2, $M_X < 1.7$ GeV	0.497	0.528	0.609	0.617	0.598	0.482	0.494	0.480	0.516
$q^2 > 11$ GeV^2, $M_X < 1.5$ GeV	0.308	0.317	0.348	0.347	0.346	0.321	0.283	0.297	0.319
$q^2 > (M_B - M_{D^*})^2$	0.283	0.293	0.329	0.338	0.318	0.298	0.257	0.273	0.293
$q^2 > (M_B - M_D)^2$	0.331	0.344	0.393	0.410	0.377	0.342	0.307	0.319	0.343

TABLE II: Inferred partial branching fraction by region, $\Delta\mathcal{B}_{\rm region}$, with model dependence in the first column. $|V_{ub}|$ calculated from the inferred partial branching fractions with all errors in the second column. The errors on $|V_{ub}|$ are statistical, detector, $B \to X_c l\nu$ model dependence, $B \to X_u l\nu$ model dependence, and theoretical uncertainty respectively. Please note, these results do *not* come from fits in the restricted regions.

	$\Delta\mathcal{B}_{\rm region} \pm$ $b \to u$ Model Error	$\lvert V_{ub}\rvert \pm$ Stat $\pm$ Detector $\pm$ $b \to c$ $\pm$ $b \to u$ $\pm$ Theory
Total $\mathcal{B}(B \to X_u l\nu)$	$(1.546 \pm 0.743) \times 10^{-3}$	$(3.82 \pm 0.17 \pm 0.55 \pm 0.23 \pm 0.92 \pm 0.12) \times 10^{-3}$
$q^2 > 6$ GeV^2, $M_X < M_D$	$(0.720 \pm 0.138) \times 10^{-3}$	$(3.84 \pm 0.17 \pm 0.55 \pm 0.23 \pm 0.37 \pm 0.31) \times 10^{-3}$
$q^2 > 8$ GeV^2, $M_X < 1.7$ GeV	$(0.548 \pm 0.069) \times 10^{-3}$	$(3.98 \pm 0.18 \pm 0.57 \pm 0.24 \pm 0.25 \pm 0.38) \times 10^{-3}$
$q^2 > 11$ GeV^2, $M_X < 1.5$ GeV	$(0.315 \pm 0.032) \times 10^{-3}$	$(4.05 \pm 0.18 \pm 0.58 \pm 0.25 \pm 0.21 \pm 0.56) \times 10^{-3}$
$q^2 > (M_B - M_{D^*})^2$	$(0.297 \pm 0.041) \times 10^{-3}$	$(4.07 \pm 0.18 \pm 0.58 \pm 0.25 \pm 0.28 \pm 0.62) \times 10^{-3}$
$q^2 > (M_B - M_D)^2$	$(0.359 \pm 0.052) \times 10^{-3}$	$(4.05 \pm 0.18 \pm 0.58 \pm 0.25 \pm 0.29 \pm 0.54) \times 10^{-3}$

V. CONCLUSION

We have made a preliminary measurement the CKM parameter $|V_{ub}|$ with high precision, but some model dependence, and obtain

$$V_{ub} \; = \; (4.05 \pm 0.18 \pm 0.58 \pm 0.25 \pm 0.21 \pm 0.56) \times 10^{-3}$$

where the errors are statistical, detector systematics, $B \to X_c l\nu$ model dependence, $B \to X_u l\nu$ model dependence, and theoretical uncertainty respectively. The result is consistent with the CLEO result using the lepton end-point measurement [5]. There is some statistical correlation with the lepton end-point measurement and the model dependence may be correlated as well. These correlations will be investigated. This analysis is the first to use neutrino reconstruction and the full three-dimensional kinematic information to extract the $B \to X_u l\nu$ branching fraction. This also pioneers the application of the multidimensional cuts laid out by Bauer *et al.*[4]. A more detailed study of the region of sensitivity is in progress, and may result in a less model dependent extraction of $|V_{ub}|$.

The composition of the $B \to X_c l\nu$ is also currently being analyzed and will provide new information on the branching fractions, the HQET parameters $\overline{\Lambda}$ and λ_1, and the Standard Model parameter $|V_{cb}|$.

We gratefully acknowledge the contributions of the CESR staff for providing the luminosity and the National Science Foundation and U.S. Department of Energy for supporting this research.

---

[1] J. Chay, H. Georgi and B. Grinstein, Phys. Lett. B **247**, 399 (1990); I. I. Bigi, M. A. Shifman, N. G. Uraltsev and A. I. Vainshtein, Phys. Rev. Lett. **71**, 496 (1993) [arXiv:hep-ph/9304225]; A. V. Manohar and M. B. Wise, Phys. Rev. D **49**, 1310 (1994); C. W. Bauer, Z. Ligeti and M. E. Luke, Phys. Lett. B **479**, 395 (2000).

[2] A. F. Falk, Z. Ligeti and M. B. Wise, Phys. Lett. B **406**, 225 (1997) [arXiv:hep-ph/9705235].

[3] M. Neubert, JHEP **0007**, 022 (2000) [arXiv:hep-ph/0006068]; M. Neubert and T. Becher, Phys. Lett. B **535**, 127 (2002) [arXiv:hep-ph/0105217].

[4] C. W. Bauer, Z. Ligeti and M. E. Luke, Phys. Rev. D **64**, 113004 (2001).

[5] A. Bornheim *et al.* [CLEO Collaboration], Phys. Rev. Lett. **88**, 231803 (2002) [arXiv:hep-ex/0202019].

[6] R. Fulton *et al.* [CLEO Collaboration], Phys. Rev. Lett. **64**, 16 (1990).

[7] Y. Kubota *et al.*, Nucl. Instrum. Meth. A **320**, 66 (1992); T. S. Hill, Nucl. Instrum. Meth. A **418**, 32 (1998).

[8] G. C. Fox and S. Wolfram, Phys. Rev. Lett. **41**, 1581 (1978).

[9] R. J. Barlow and C. Beeston, Comput. Phys. Commun. **77**, 219 (1993).

[10] D. Scora and N. Isgur, Phys. Rev. D **52**, 2783 (1995) [arXiv:hep-ph/9503486].

[11] J. E. Duboscq *et al.* [CLEO Collaboration], Phys. Rev. Lett. **76**, 3898 (1996).

[12] J. L. Goity and W. Roberts, Phys. Rev. D **51**, 3459 (1995) [arXiv:hep-ph/9406236].

[13] W. Bacino *et al.*, Phys. Rev. Lett. **43**, 1073 (1979).

[14] A. H. Hoang, Z. Ligeti and A. V. Manohar, Phys. Rev. D **59**, 074017 (1999) [arXiv:hep-ph/9811239]; N. Uraltsev, Int. J. Mod. Phys. A **14**, 4641 (1999) [arXiv:hep-ph/9905520].